

Regulation of Cell Adhesion Free Energy by External Sliding Forces

T. Yang · M.H. Zaman

Received: 2 April 2007 / Accepted: 25 October 2007
© Society for Experimental Mechanics 2007

Abstract Cells experience a variety of forces and external velocities *in vivo*. While a number of continuum based models have addressed cell substrate interactions in these dynamic environments, a molecular picture of adhesion under external sliding forces and velocities is lacking. Using a molecular thermodynamic model, that incorporates entropic and steric repulsions, molecular conformations and constraints, penetrable substrates and explicit binding interactions, we study the effect of external sliding velocities on cell adhesion. We map the free energy landscapes under a broad range of external forces, binding energies and receptor surface coverages. Our calculations predict the regimes where free energy landscapes become resistant to external forces. Our model shows good agreement with experimental studies and lays out a scalable framework for analyzing and quantifying a broad spectrum of *in vivo* and *in vitro* adhesion studies.

Keywords Cell–matrix adhesion · Adhesion force · Free energy

Introduction

Cell adhesion affects a variety of cellular and multi-cellular processes. These process control cell proliferation, cell migration, signaling and apoptosis [1–7]. Additionally, differentiation of stem cells shows a strong dependence upon mechano-chemical interactions with the substrate [8]. Our ability to design, modify and characterize substrates optimized for specific adhesion applications depends upon a thorough and quantitative understanding of cell substrate interactions.

A number of computational and experimental studies have focused on quantifying cell matrix interactions, in particular cell adhesion [5, 9–23]. The experimental studies have utilized state of the art techniques to understand both the biochemical and biomechanical aspects of cell adhesion. These studies have provided a wealth of knowledge about forces, stresses and other mechano-chemical interactions at the cell–substrate interface. In a similar fashion, a number of theoretical endeavors have also given deeper insights into cell adhesion in particular, and cell matrix interactions in general [9, 24–33]. Theoretical studies have investigated the role of substrate rigidity, cellular stiffness and cytoskeletal mechanics in regulating adhesion and migration. Computational studies have also probed a number of key questions in cell adhesion that are currently beyond the reach of experiments. While computational models have provided useful insights into cell adhesion and migration, most models have focused exclusively at the continuum level. This lack of molecular detail has unfortunately limited the applicability of these models to a subset of *in vivo* and *in vitro* experiments.

Using molecular models that incorporate conformational preferences, entropic repulsion and solvent effects, we have previously quantified cell adhesion in terms of a number of

T. Yang
Department of Physics,
The University of Texas at Austin,
Austin, TX 78712, USA

M.H. Zaman (✉)
Department of Biomedical Engineering
and Institute of Theoretical Chemistry,
The University of Texas at Austin,
Austin, TX 78712, USA
e-mail: mhzaman@mail.utexas.edu

thermodynamic and statistical parameters [34] (Yang and Zaman, submitted for publication). Our novel geometry independent models have predicted the effects of conformational restriction, receptor asymmetry and substrate chemistry on free energy and adhesion force. However, these models have not probed the effect of external force on overall adhesion. Cells adhere and interact with substrates in dynamic mechano-chemical environments and are subjected to a number of external forces. In this paper, we develop and implement a computational strategy to calculate free energy of a cell experiencing external sliding velocities. Our model addresses binding and unbinding interactions in the presence of external velocities and quantifies adhesion force as a function of the magnitude of external velocity, surface coverage of adhesion receptors and the strength of binding interaction. We believe that our calculations of in realistic dynamic environments will provide a molecular level understanding of adhesion *in vivo* and *in vitro*. In addition, models such as ours will provide design strategies for next generation of biomaterials that are optimized for specific pharmaceutical and biotechnological applications.

Methods

A schematic of the cell–substrate system used in this study is shown in Fig. 1. The system consists of a cell, with its bottom membrane containing receptors, and a bottom “box” represents a penetrable adhesive substrate (Table 1). The reason to use a “penetrable” adhesive box instead of a single plate is to capture realistic scenarios in numerous experimental studies. A large number of cell adhesion studies use collagen or Matrigel gels as substrates. These

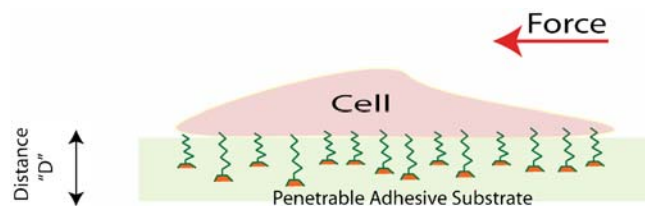


Fig. 1 A cartoon depicting the system studied in our calculations. The external force acts on the surface (membrane) decorated with adhesion receptors. The conformations of the adhesion receptors are computed by coarse-grained simulations that account for backbone torsions and side chain sterics. The receptors interact with a penetrable adhesive substrate of finite thickness. The free energy of interaction consists of three key terms, namely binding interactions, solvent incompressibility and conformational entropy due to the receptors. The free energies are computed as a function of distance between the cell membrane and the far end of the adhesive substrate. The change in free energy as a function of distance allows us to calculate adhesion force

Table 1 Table of symbols used in the model with appropriate units

Symbol	Quantity	Unit
z	Coordinate in the direction normal to membrane	M
T	Temperature	K
v_s	VDW volume of solvent molecule	m^3
v	VDW volume of monomer	m^3
S	Area of membrane	m^2
N	Number of receptors	Dimensionless
σ	Surface coverage (N/S)	m^{-2}
δ	Thickness of one layer	M
σ'	Dimensionless surface coverage ($\sigma v/\delta$)	Dimensionless
A	Free energy	J
a	$A/k_B T S$	m^{-2}
D	Separation	M
$\delta(\alpha)$	Conformation dependent interaction function	Dimensionless
e	Bond energy	$k_B T$
e'	Dimensionless bond energy ($e/k_B T$)	Dimensionless
V	Sliding velocity	m/s
$P(V, e)$	Velocity and energy dependent bonding probability	Dimensionless
P_α	Probability of receptor's α th conformation	Dimensionless
$\varphi_s(z)$	Volume fraction of solvent	Dimensionless
$n_{R\alpha}(z)$	Number density of the α th conformation at z	m^{-1}
$f_l(z)$	Volume fraction of ligands	Dimensionless
$f(z)$	$1-f_l(z)$	Dimensionless
$x(z)$	Dimensionless osmotic pressure	Dimensionless
f	Average force exerted on one monomer	N
λ	Average distance between neighboring monomers	M
k_0	Rate of reaction in absence of external force	s^{-1}
k_f	Forward reaction rate in presence of external force	s^{-1}
k_b	Backward reaction rate in presence of external force	s^{-1}
N_b	Number of receptors in bonding state	Dimensionless
N_f	Number of receptors in free state	Dimensionless

VDW = van der Waals

substrates are of finite thickness and are penetrable by solvent molecules and cell adhesion receptors.

The cell membrane is decorated with receptors with a uniform surface coverage σ . The conformations of the receptors are generated by simulating the allowed ϕ/ψ angles of the integrin amino acids. The receptors are 150 amino acids long and the side chains are simulated through a hard-sphere model as described elsewhere [34]. Our simulations are superior to simple hard sphere simulations

that do not account for the backbone torsion angles or the side chains. For simplicity, we assume that only the terminal region (last 20 amino acids) of the receptor interacts with the ligands and the other regions of the receptors that are chemically inert. This is a reasonable approximation given that integrins bind to ligands at specific locations on the molecular surface [34]. The penetrable adhesive substrate is assumed to contain receptor binding ligands that interact with the receptors with a binding energy “ e ”.

To capture the effect of *in vivo* scenarios, where a cell is subjected to external velocities and forces, we introduce constant sliding velocity acting on the cell membrane. The receptors are distributed in the z direction within 10 nm from the cell membrane. The adhesive box is assumed to have a fixed height of 8 nm along the z direction. If the binding region (i.e. last 20 amino acids) of the receptor does not overlap with the substrate (adhesive box), there is no receptor–substrate binding. Receptors that go inside the box are regarded as potentially binding receptors. This means that not all potentially binding receptors form bonds with ligands. The possibility for a bond between a receptor and a ligand is related to the sliding velocity and bond energy. This issue is discussed in detail in the later part of this section. First, we describe our method to compute the free energy of the system of interest.

The free energy can be written as:

$$A = k_B T N \sum_{\{\alpha\}} P_\alpha \ln P_\alpha + \frac{k_B T S}{v_s} \int dz \varphi_s(z) \ln \varphi_s(z) - e P(V, e) N \sum_{\{\alpha\}} P_\alpha \delta(\alpha) \quad (1)$$

in which, A is the free energy of the system. The first term in equation (1) comes from the entropy of receptors where k_B is the Boltzmann constant, T is the temperature of the system and N is the total number of receptors. α denotes the conformation of receptors and P_α is the probability of finding the conformation α of all receptors. The second term in equation (1) is rooted in the translational entropy of solvent molecules, in which “ S ” is the total area of the membrane, v_s is the Van der Waals volume of solvent molecule and $\varphi_s(z)$ is the volume fraction of solvent in the layer ($z, z+dz$). The last term refers to the specific binding energy of receptors and ligands, in which “ e ” is the bond energy. The term $N \sum_{\{\alpha\}} P_\alpha \delta(\alpha)$ is the number of potentially binding receptors with $\delta(\alpha)$ equal to 1 if the α th conformation has overlap with the box and 0 otherwise. $P(V, e)$ is the conditional probability for a potentially binding receptor to make a bond which depends on velocity and bond energy.

Dividing equation (1) by $k_B T S$, we arrive at:

$$a := \frac{A}{k_B T S} = \sigma \sum_{\{\alpha\}} P_\alpha \ln P_\alpha + \frac{1}{v_s} \int dz \varphi_s(z) \ln \varphi_s(z) - \sigma e' P(V, e) \sum_{\{\alpha\}} P_\alpha \delta(\alpha) \quad (2)$$

Where $\sigma := \frac{N}{S}$ is the surface coverage of receptors. $e' := \frac{e}{kT}$ is dimensionless binding energy. The short-term strong repulsion between the monomers and the solvent is accounted for through packing constraints. In the layer ($z, z+dz$), the packing constraint is formulated as:

$$\langle \varphi_R(z) \rangle + \varphi_s(z) = 1 - f_L(z) \quad (3)$$

in which, $\langle \rangle$ denotes ensemble average over all conformations. Hence $\langle \varphi_R(z) \rangle$ is the volume fraction of receptors in ($z, z+dz$), which can be expressed as:

$$\langle \varphi_R(z) \rangle = \frac{N \langle n_R(z) \rangle dz v}{S dz} = \sigma v \sum_{\{\alpha\}} P_\alpha n_{R\alpha}(z) \quad (4)$$

where $\langle n_R(z) \rangle dz$ is the ensemble averaged number of segments of receptor in ($z, z+dz$), v is the Van der Waals volume of the monomer. In equation (4), $n_{R\alpha}(z)$ is the number density of segments of the α th conformation of receptor, which is derived from the sampling of receptors. $f_L(z)$ is the volume fraction of ligands in the box at z , which is either zero in the case the box is beyond z or a constant number otherwise. For our purposes, the constant value is assumed to be as 0.05. We define $f(z) := 1 - f_L(z)$. The constraint equation now becomes:

$$\sigma v \sum_{\{\alpha\}} P_\alpha n_{R\alpha}(z) + \varphi_s(z) = f(z) \quad (5)$$

In order to calculate the free energy, we minimize the quantity “ a ” in equation (2) with respect to the pdf P_α and the solvent term $\varphi_s(z)$. We introduce a Lagrangian multiplier $x(z)$ in the constraint equation. The physical interpretation of $x(z)$ is dimensionless osmotic pressure. The simultaneous equations can now be written as:

$$P_\alpha = \frac{1}{g_R} \exp \left(- \int dz x(z) n_{R\alpha}(z) + e' P(V, e) \delta(\alpha) \right) \quad (6)$$

$$\varphi_s(z) = \exp(-x(z)) \quad (7)$$

$$\sigma v \sum_{\{\alpha\}} P_\alpha n_{R\alpha}(z) + \exp(-x(z)) = f(z) \quad (8)$$

In equation (6), $g_R := \sum_{\{\alpha\}} \exp(-\int dx(r) n_{R\alpha}(r)) e' P(V, e) \delta(\alpha)$ is the partition function to normalize the pdf P_α . Equations (6), (7) and (8) represent a closed set of equations. Taking

segment number density $n_{R\alpha}(z)$, the fraction of solvent and receptors $f(z)$ and binding potentiality $\delta(\alpha)$ as input, surface coverage σ , binding energy e' and sliding velocity V as parameters, we can calculate the free energies at a series of separations between the membrane and the far edge of the box.

As we vary the distance between the cell and the substrate, the total number of layers change as do the numbers of monomers of receptors in layers $n_{R\alpha}(i)$. In addition the fraction $f(z)$, the number of receptors potentially binding may also change, therefore changing the net free energy.

To solve the simultaneous equations above, we follow the method of I. Szleifer and co-workers [35–39]. The horizontal x–y plane is assumed to be homogeneous. The space between the membrane and far edge of the box is sliced into layers along z direction, denoted as i . The solution is derived by iterating the equations below:

$$P_{\alpha}^n = \frac{1}{g_R^n} \exp \left(- \sum_i x^{n-1}(i) n_{R\alpha}(i) + P(V, e') e' \delta(\alpha) \right) \quad (9)$$

$$x^n(i) = - \ln \left(f(i) - \sigma' \sum_{\{\alpha\}} P_{R\alpha}^n n_{R\alpha}(i) \right) \quad (10)$$

where the superscript denotes the order of iteration, $\sigma' := \frac{\sigma V}{\delta}$ is the dimensionless surface coverage and δ is the thickness of one layer (taken as 0.5 nm).

Finally, we address the binding probability as a function of relative velocity and binding energy. Assuming a mechanical force balance in the translational plane, the average force exerted on a monomer is f , the average distance between neighboring monomers or that between monomer and solvent molecules is λ . Eyring [40, 41] showed that if k_0 is the reaction rate in the absence of an external force, k_f is the rate along the forward direction when there is a microscopic force f . And similarly, k_b is the rate of backward reaction. In the presence of an external microscopic force, these rates are given by:

$$k_f = k_0 \exp \left(\frac{f\lambda}{2k_B T} \right) \quad (11)$$

$$k_b = k_0 \exp \left(- \frac{f\lambda}{2k_B T} \right) \quad (12)$$

We can relate the microscopic force f with the macroscopic velocity V by

$$V = \lambda k_0 \left(\exp \left(\frac{f\lambda}{2k_B T} \right) - \exp \left(- \frac{f\lambda}{2k_B T} \right) \right) \quad (13)$$

We assume that the binding and unbinding of receptors and ligands is a kinetic process of a two energy states

system. At equilibrium, the number of potentially binding receptors is given by N' , among which, N_b are receptors in the binding state, N_f are in the free state. Due to the presence of an external force f , the energy difference between the two states is lowered to $N_b/N_f = \exp((e - f\lambda/2)/k_B T)$.

Therefore,

$$P(f, e') = 1 - \frac{1}{1 + \exp \left(e' - \frac{f\lambda}{2k_B T} \right)} \quad (14)$$

From equations (13) and (14), we get $P(V, e')$, which describes the probabilities in an external velocity framework. In this paper we assume $k_0=10/s$ and $\lambda=0.3$ nm.

Results

In order to quantify the effect of external sliding force on cell adhesion, we first study the effect of external velocity on binding and unbinding. Figure 2 shows the effect of the magnitude of external velocity on percentage of bonds remaining as a function of binding energy. The percentage is calculated by comparing the number of available bonds to the number of bonds formed in the absence of any external sliding velocity. Our results show that at high binding interactions (such as $e=10 k_B T$), even very high velocities, such as 1 $\mu\text{m/s}$ do not lead to any significant bond breakage and the cell remains strongly adhered. On the other hand, as the adhesion energy decreases, increasing sliding velocities leads to only a small fraction of bonds forming.

The percentage of available bonds allows us to map the free energy landscape of cell adhesion in the presence of

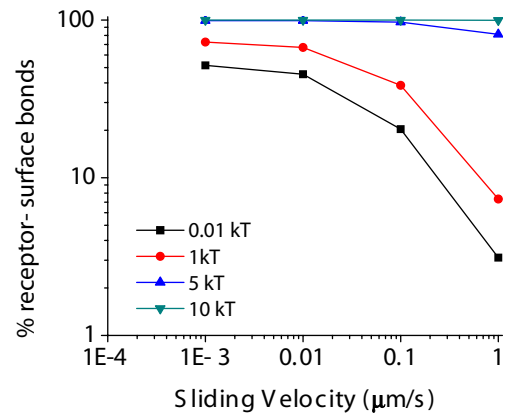
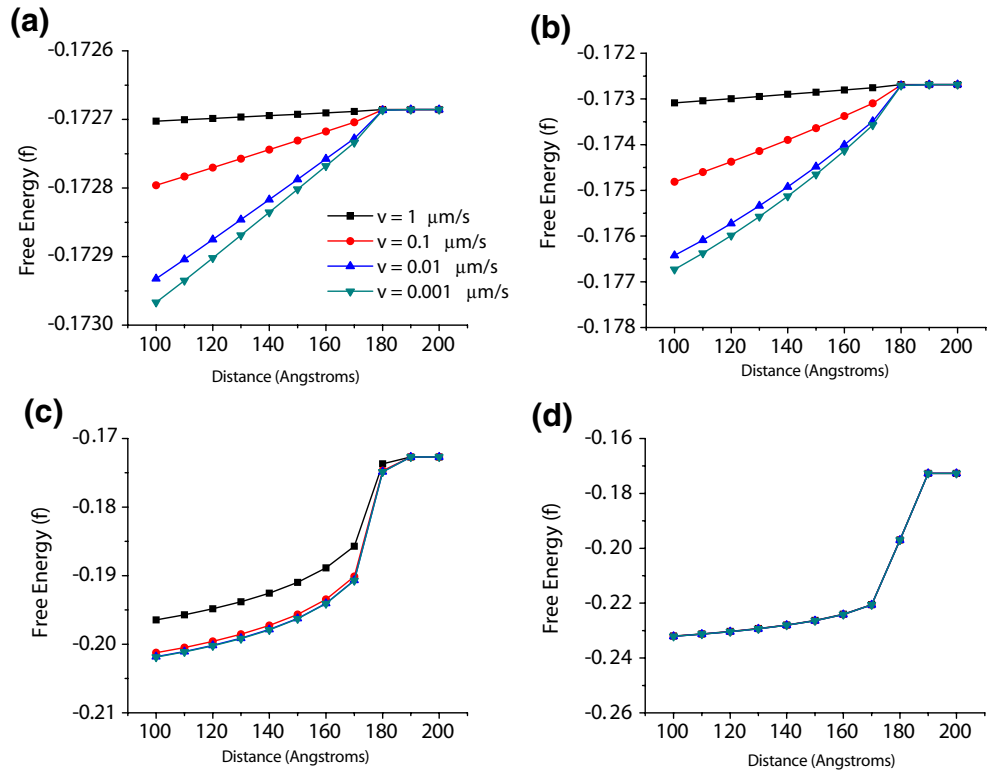


Fig. 2 The percentage of bonds between the cell and the substrate vary with the magnitude of external velocity and the strength of the binding interactions. At lower speeds and high interaction energies, most bonds remain intact. However, at high speeds and lower binding energies, the number of bonds formed is a small fraction of the total number of bonds formed in the absence of any external forces

Fig. 3 The free energies of cell substrate adhesion at four different binding energies. At $0.1 k_B T$, the free energy of the system at high velocities is fairly high and the system remains unstable (a). The gap between free energies at various velocities starts to decrease as the binding interaction increases to $1 k_B T$ (b). At even higher binding interactions [(c); $e=5 k_B T$] the gap between free energies at lower and higher velocities is very small. At $e=10 k_B T$ (d), the free energy landscape is invariant to external velocities. This is because even high sliding velocities are unable to cause any significant loss in binding

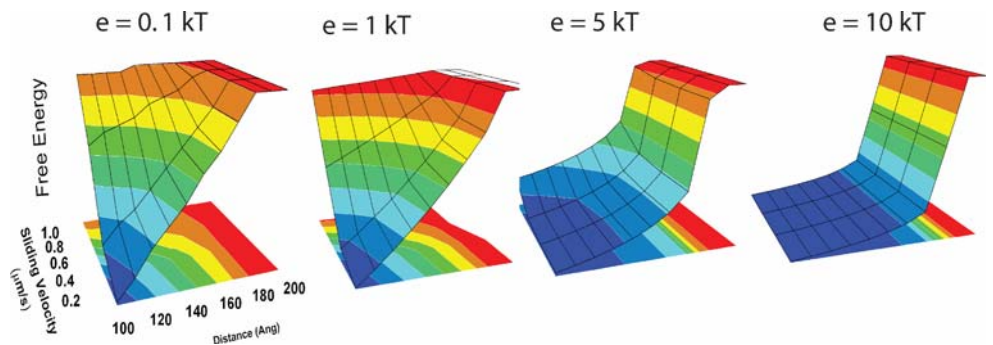


external sliding velocity. Figure 3 shows the effects of adhesion binding energy and sliding velocity on overall free energy of adhesion. The results are shown for a given surface coverage (0.01). Results for other surface coverages are qualitatively similar and differ only in magnitude. Our results show a number of key features that have not been quantified previously through continuum level models. First of all, we note that at lowest interaction energy [Fig. 3(a)], cell adhesion is most stable at lowest speeds and short distances between the substrate and the cell. As the sliding velocity increases, there are only a few bonds formed between the surface and the cell, as a result increasing free energy does not change the free energy landscape significantly. In other words, for a weakly interacting system, high velocities produce no significant change in the free energy landscape. On the other hand, for

these weakly interacting systems, lower velocities have smaller effect at shorter distances, but as the separation increases, the free energy starts to increase. This is because fewer bonds are formed at greater distances and even smaller velocities are able to disrupt these bonds. Thus for a weakly interacting system, higher speeds show smaller changes in the free energy landscape as a function of distance, while lower speeds show a stable system at shorter distance but approach instabilities caused by higher velocities at greater distances.

As the interaction energy is increased by an order of magnitude, we note that the gap between lower and higher velocities starts to decrease. This pattern is observed as we increase the cell substrate binding further, first to $5 k_B T$ and $10 k_B T$. With increasing binding energy, the free energy landscape becomes less and less responsive to changes in

Fig. 4 The free energy landscape at various binding interactions is shown. As the binding energy increases, the free energy landscape becomes smooth and resistant to external sliding velocities



velocity. At $10 k_B T$, the velocity has virtually no effect at all on the overall free energy landscape. This result may seem counterintuitive, but in fact can be explained by the trends observed in Fig. 2. As the interaction energy increases, the effect of external velocity reduces. As shown in Fig. 2, at $10 k_B T$, even $1 \mu\text{m/s}$ does not lead to any significant unbinding. As a result, the system shows invariance to external sliding. This invariance results in the robustness of the free energy landscape, and the free energy profile of the system remains the same regardless of external velocities.

The dynamics of the free energy landscape are captured in Fig. 4 that shows the variations in the landscape as a function of binding interactions. The 3D plots demonstrate the free energy variations as a function of distance and sliding velocities. As suggested by Fig. 4, the landscape becomes increasingly smooth as the interaction energy increases. Landscape plots such as the ones depicted in Fig. 4 provide useful insights into the robustness and resistance of a system to external forces.

Discussion and Conclusions

Cell–substrate interactions have tremendous significance in tissue engineering, biomaterial design and pharmaceutical industries. A detailed description of these interactions will allow us to design and optimize next generation of smart biomaterials. Using a molecular thermodynamic model, we have quantified the effect of external sliding velocity on the magnitude of free energy and adhesion force in cell substrate interactions. Our model incorporates steric entropic effects of the receptor chains, solvent incompressibility and predicts adhesion free energies as a function of the strength of binding interactions. Our model also maps the dynamic landscape of adhesion free energy in the presence of external sliding force and quantifies regimes for maximum and minimum adhesion.

The predictions of our model show good agreement with existing experimental studies [42–47]. First of all, our model does not incorporate the chemical effects of the solvent that will affect binding and unbinding interactions. In addition, the forward and reverse reaction rates used in our model may also be averaged parameters and vary for various cell types. Finally, the surface coverage of integrin receptors used in our model may also be on the higher end of experiment values for integrins available for binding at any given time. In spite of these limitations, our model is a first of its kind study to quantify the effects of sliding velocities on cell adhesion while incorporating molecular thermodynamic aspects of cell adhesion. Our current framework lays the foundation for future models that will incorporate biochemical, biophysical and biomechanical features of cell adhesion receptors and their ligands in quantifying the

molecular and cellular response to forces experienced by cells. Such models will aid researchers, both in experimental and computational bioengineering to further understand the molecular basis of cell adhesion and to quantify cell adhesion in a variety of *in vivo* settings.

Acknowledgements This work was supported in part by Robert A. Welch Foundation grant to MHZ and by faculty development startup funds provided to MHZ from the Department of Biomedical Engineering and Cockrell School of Engineering at UT Austin.

References

1. Lauffenburger DA, Horwitz AF (1996) Cell migration: a physically integrated molecular process. *Cell* 84:359–369.
2. Critchley DR (2000) Focal adhesions—the cytoskeletal connection. *Curr Opin Cell Biol* 12:133–139.
3. Ridley AJ, Schwartz MA, Burridge K, Firtel RA, Ginsberg MH, Borisy G, Parsons JT, Horwitz AR (2003) Cell migration: integrating signals from front to back. *Science* 302:1704–1709.
4. Hynes RO, Zhao Q (2000) The evolution of cell adhesion. *J Cell Biol* 150:F89–F96.
5. Petit V, Thiery JP (2000) Focal adhesions: structure and dynamics. *Biol Cell* 92:477–494.
6. Hynes RO (2002) Integrins: bidirectional, allosteric signaling machines. *Cell* 110:673–687.
7. Hynes RO (1987) Integrins: a family of cell surface receptors. *Cell* 48:549–554.
8. Engler AJ, Sen S, Sweeney HL, Discher DE (2006) Matrix elasticity directs stem cell lineage specification. *Cell* 126:677–689.
9. Hammer DA, Tempelman LA, Apte SM (1993) Statistics of cell adhesion under hydrodynamic flow: simulation and experiment. *Blood Cells* 19:261–275; discussion 275–267.
10. Wu P, Hoying JB, Williams SK, Kozikowski BA, Lauffenburger DA (1994) Integrin-binding peptide in solution inhibits or enhances endothelial cell migration, predictably from cell adhesion. *Ann Biomed Eng* 22:144–152.
11. O'Brien FJ, Harley BA, Yannas IV, Gibson LJ (2005) The effect of pore size on cell adhesion in collagen-GAG scaffolds. *Biomaterials* 26:433–441.
12. Yauch RL, Felsenfeld DP, Kraeft SK, Chen LB, Sheetz MP, Hemler ME (1997) Mutational evidence for control of cell adhesion through integrin diffusion/clustering, independent of ligand binding. *J Exp Med* 186:1347–1355.
13. Kornberg L, Earp HS, Parsons JT, Schaller M, Juliano RL (1992) Cell adhesion or integrin clustering increases phosphorylation of a focal adhesion-associated tyrosine kinase. *J Biol Chem* 267:23439–23442.
14. Paku S, Tovari J, Lorincz Z, Timar F, Dome B, Kopper L, Raz A, Timar J (2003) Adhesion dynamics and cytoskeletal structure of gliding human fibrosarcoma cells: a hypothetical model of cell migration. *Exp Cell Res* 290:246–253.
15. Pichard V, Honore S, Kovacic H, Li C, Prevot C, Briand C, Rognoni JB (2001) Adhesion, actin cytoskeleton organisation and the spreading of colon adenocarcinoma cells induced by EGF are mediated by alpha2beta1 integrin low clustering through focal adhesion kinase. *Histochem Cell Biol* 116:337–348.
16. Munevar S, Wang YL, Dembo M (2001) Distinct roles of frontal and rear cell–substrate adhesions in fibroblast migration. *Mol Biol Cell* 12:3947–3954.

17. Cukierman E, Pankov R, Stevens DR, Yamada KM (2001) Taking cell–matrix adhesions to the third dimension. *Science* 294:1708–1712.
18. Burgess BT, Myles JL, Dickinson RB (2000) Quantitative analysis of adhesion-mediated cell migration in three-dimensional gels of RGD-grafted collagen. *Ann Biomed Eng* 28:110–118.
19. Smilenov LB, Mikhailov A, Pelham RJ, Marcantonio EE, Gundersen GG (1999) Focal adhesion motility revealed in stationary fibroblasts. *Science* 286:1172–1174.
20. Pelham RJ Jr, Wang Y (1997) Cell locomotion and focal adhesions are regulated by substrate flexibility. *Proc Natl Acad Sci U S A* 94:13661–13665.
21. Kuntz RM, Saltzman WM (1997) Neutrophil motility in extracellular matrix gels: mesh size and adhesion affect speed of migration. *Biophys J* 72:1472–1480.
22. Kuo SC, Lauffenburger DA (1993) Relationship between receptor/ligand binding affinity and adhesion strength. *Biophys J* 65:2191–2200.
23. Ward MD, Hammer DA (1992) Morphology of cell–substratum adhesion. Influence of receptor heterogeneity and nonspecific forces. *Cell Biophys* 20:177–222.
24. Civelekoglu-Scholey G, Orr AW, Novak I, Meister JJ, Schwartz MA, Mogilner A (2005) Model of coupled transient changes of Rac, Rho, adhesions and stress fibers alignment in endothelial cells responding to shear stress. *J Theor Biol* 232:569–585.
25. Brinkerhoff CJ, Linderman JJ (2005) Integrin dimerization and ligand organization: key components in integrin clustering for cell adhesion. *Tissue Eng* 11:865–876.
26. Irvine DJ, Hue KA, Mayes AM, Griffith LG (2002) Simulations of cell-surface integrin binding to nanoscale-clustered adhesion ligands. *Biophys J* 82:120–132.
27. Palecek SP, Horwitz AF, Lauffenburger DA (1999) Kinetic model for integrin-mediated adhesion release during cell migration. *Ann Biomed Eng* 27:219–235.
28. Dickinson RB, Tranquillo RT (1993) A stochastic model for adhesion-mediated cell random motility and haptotaxis. *J Math Biol* 31:563–600.
29. Hammer DA, Apte SM (1992) Simulation of cell rolling and adhesion on surfaces in shear flow: general results and analysis of selectin-mediated neutrophil adhesion. *Biophys J* 63:35–57.
30. DiMilla PA, Barbee K, Lauffenburger DA (1991) Mathematical model for the effects of adhesion and mechanics on cell migration speed. *Biophys J* 60:15–37.
31. Hammer DA, Lauffenburger DA (1989) A dynamical model for receptor-mediated cell adhesion to surfaces in viscous shear flow. *Cell Biophys* 14:139–173.
32. Dembo M, Torney DC, Saxman K, Hammer D (1988) The reaction-limited kinetics of membrane-to-surface adhesion and detachment. *Proc R Soc Lond B Biol Sci* 234:55–83.
33. Hammer DA, Lauffenburger DA (1987) A dynamical model for receptor-mediated cell adhesion to surfaces. *Biophys J* 52:475–487.
34. Yang T, Zaman MH (2007) Free energy landscape of receptor mediated cell adhesion. *J Chem Phys* 126:045103.
35. Longo G, Szleifer I (2005) Ligand-receptor interactions in tethered polymer layers. *Langmuir* 21:11342–11351.
36. Huang YB, Szleifer I, Peppas NA (2002) A molecular theory of polymer gels. *Macromolecules* 35:1373–1380.
37. Huang YB, Szleifer I, Peppas NA (2001) Gel–gel adhesion by tethered polymers. *J Chem Phys* 114:3809–3816.
38. Szleifer I, Carignano MA (1996) Tethered polymer layers. *Adv Chem Phys Xciv* 94:165–260.
39. Carignano MA, Szleifer I (1993) Statistical thermodynamic theory of grafted polymeric layers. *J Chem Phys* 98:5006–5018.
40. Eyring H (1938) Viscosity, plasticity, diffusion as examples of absolute reaction rates. *J Chem Phys* 4:238–241.
41. Eyring H (1935) The activated complex in chemical reactions. *J Chem Phys* 3:107–115.
42. Zamir E, Katz M, Posen Y, Erez N, Yamada KM, Katz BZ, Lin S, Lin DC, Bershadsky A, Kam Z, Geiger B (2000) Dynamics and segregation of cell–matrix adhesions in cultured fibroblasts. *Nat Cell Biol* 2:191–196.
43. Sun Z, Martinez-Lemus LA, Trache A, Trzeciakowski JP, Davis GE, Pohl U, Meininger GA (2005) Mechanical properties of the interaction between fibronectin and alpha5beta1-integrin on vascular smooth muscle cells studied using atomic force microscopy. *Am J Physiol* 289:H2526–H2535.
44. Trache A, Trzeciakowski JP, Gardiner L, Sun Z, Muthuchamy M, Guo M, Yuan SY, Meininger GA (2005) Histamine effects on endothelial cell fibronectin interaction studied by atomic force microscopy. *Biophys J* 89:2888–2898.
45. Bershadsky AD, Balaban NQ, Geiger B (2003) Adhesion-dependent cell mechanosensitivity. *Annu Rev Cell Dev Biol* 19:677–695.
46. Schwarz US, Balaban NQ, Rivelino D, Bershadsky A, Geiger B, Safran SA (2002) Calculation of forces at focal adhesions from elastic substrate data: the effect of localized force and the need for regularization. *Biophys J* 83:1380–1394.
47. Balaban NQ, Schwarz US, Rivelino D, Goichberg P, Tzur G, Sabanay I, Mahalu D, Safran S, Bershadsky A, Addadi L, Geiger B (2001) Force and focal adhesion assembly: a close relationship studied using elastic micropatterned substrates. *Nat Cell Biol* 3:466–472.